This article is a *Plant Cell* Advance Online Publication. The date of its first appearance online is the official date of publication. The article has been edited and the authors have corrected proofs, but minor changes could be made before the final version is published. Posting this version online reduces the time to publication by several weeks.

Arabidopsis CSN5B Interacts with VTC1 and Modulates Ascorbic Acid Synthesis[W]

Juan Wang,[a,b] Yanwen Yu,[a,b] Zhijin Zhang,[a,b] Ruidang Quan,[a,b] Haiwen Zhang,[a,b] Ligeng Ma,[c] Xing Wang Deng,[d,1] and Rongfeng Huang[a,b,1,2]

[a] Biotechnology Research Institute, Chinese Academy of Agricultural Sciences, Beijing 100081, China
[b] National Key Facility of Crop Gene Resources and Genetic Improvement, Beijing 100081, China
[c] College of Life Sciences, Capital Normal University, Beijing 100048, China
[d] Department of Molecular, Cellular, and Developmental Biology, Yale University, New Haven, Connecticut 06520-8104

Light regulates ascorbic acid (AsA) synthesis, which increases in the light, presumably reflecting a need for antioxidants to detoxify reactive molecules produced during photosynthesis. Here, we examine this regulation in *Arabidopsis thaliana* and find that alterations in the protein levels of the AsA biosynthetic enzyme GDP-Man pyrophosphorylase (VTC1) are associated with changes in AsA contents in light and darkness. To find regulatory factors involved in AsA synthesis, we identified VTC1-interacting proteins by yeast two-hybrid screening of a cDNA library from etiolated seedlings. This screen identified the photomorphogenic factor COP9 signalosome subunit 5B (CSN5B), which interacted with the N terminus of VTC1 in yeast and plants. Gel filtration profiling showed that VTC1-CSN5B also associated with the COP9 signalosome complex, and this interaction promotes ubiquitination-dependent VTC1 degradation through the 26S proteasome pathway. Consistent with this, *csn5b* mutants showed very high AsA levels in both light and darkness. Also, a double mutant of *csn5b* with the partial loss-of-function mutant *vtc1-1* contained AsA levels between those of *vtc1-1* and *csn5b*, showing that CSN5B modulates AsA synthesis by affecting VTC1. In addition, the *csn5b* mutant showed higher tolerance to salt, indicating that CSN5B regulation of AsA synthesis affects the response to salt stress. Together, our data reveal a regulatory role of CSN5B in light-dark regulation of AsA synthesis.

INTRODUCTION

Ascorbic acid (AsA; vitamin C) is an important plant-derived antioxidant and constitutes a major source of dietary vitamin C in humans; in plants, AsA plays important roles in growth, development, and stress responses (Smirnoff and Wheeler, 2000; Hemavathi et al., 2010; Zhang et al., 2012). AsA has been proposed to function as an enzyme cofactor in photosynthesis and the syntheses of ethylene, gibberellins, and anthocyanins. AsA is synthesized via multiple biosynthetic pathways, including the D-glucosone (Loewus, 1999), D-galacturonate (Davey et al., 1999), *myo*-inositol (Lorence et al., 2004), and D-Man/L-Gal pathways (Wheeler et al., 1998); of these, the D-Man/L-Gal pathway is particularly important in plants (Wheeler et al., 1998; Lorence et al., 2004; Ishikawa and Shigeoka, 2008). The enzymes involved in these pathways have been identified (Imai et al., 1998; Conklin et al., 1999; Gatzek et al., 2002; Wolucka and Van Montagu, 2003; Laing et al., 2004, 2007; Dowdle et al., 2007). Mutations in the D-Man/L-Gal pathway result in significantly decreased AsA synthesis. For example, the enzyme GDP-Man pyrophosphorylase (VTC1) is involved in the D-Man/L-Gal pathway, and the mutant *vtc1-1*, which has reduced enzymatic activity, exhibits decreased AsA synthesis (Conklin et al., 1999).

Environmental signals such as light and stress can induce the expression of AsA synthesis–related genes and enhance AsA synthesis in tomato (*Solanum lycopersicum*) and *Arabidopsis thaliana* (Huang et al., 2005; Ioannidi et al., 2009). Light influences the accumulation of AsA in the leaves of *Arabidopsis*, and the leaf AsA content is light dependent, most likely because AsA plays roles in photosynthesis and photoprotection (Smirnoff, 2000). *Arabidopsis* leaves acclimated to high light contain higher AsA levels than leaves grown under a low light intensity, while the AsA content is decreased in leaves grown under dark conditions (Yabuta et al., 2007). Other studies have indicated that low-light conditions decrease the transcript levels of genes encoding AsA synthetic enzymes, including L-galactono-1,4-lactone dehydrogenase and VTC1, in tobacco (*Nicotiana tabacum*; Tabata et al., 2002), whereas high-light conditions increase the transcript level and enzymatic activity of GDP-L-Gal phosphorylase (Dowdle et al., 2007). In addition, light-responsive *cis*-elements have been found in the promoter regions of the genes encoding L-Gal-1-phosphate phosphatase and L-galactono-1,4-lactone dehydrogenase in rice (*Oryza sativa*; Fukunaga et al., 2010). Increasing evidence suggests that multiple environmental factors, including light and salt stress, affect AsA synthesis at the transcriptional level (Yabuta et al., 2007; Zhang et al., 2012). In *Arabidopsis*, the transcription of key enzymes in the AsA biosynthetic pathway (including *VTC1*) increased in the light but

[1] These authors contributed equally to this work.
[2] Address correspondence to rfhuang@caas.cn.
The author responsible for distribution of materials integral to the findings presented in this article in accordance with the policy described in the Instructions for Authors (www.plantcell.org) is: Rongfeng Huang (rfhuang@caas.cn).
[W] Online version contains Web-only data.
www.plantcell.org/cgi/doi/10.1105/tpc.112.106880

did not significantly decrease in the dark (Yabuta et al., 2007), indicating that the activities of AsA biosynthetic enzymes are posttranscriptionally modulated in the dark. However, the mechanism by which light and darkness affect AsA synthesis at the protein level is still unclear.

To identify light-related AsA biosynthetic regulators, we isolated VTC1-interacting proteins in the AsA biosynthetic pathway in *Arabidopsis*. In this report, we reveal that VTC1 interacts with a component of the photomorphogenic COP9 signalosome (CSN), CSN5B, by associating with the CSN complex. Analyses of AsA content indicated that CSN5B affects AsA biosynthesis and subsequently modulates plant responses to oxidative and salt stresses. Moreover, we found that VTC1 is degraded in vitro and in vivo in the dark through the 26S proteasome pathway, and this degradation requires CSN5B, indicating the regulatory function of the photomorphogenic factor CSN5B in AsA synthesis.

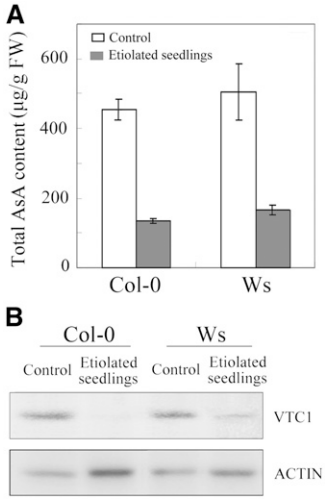

Figure 1. Reduced VTC1 Protein Production and Decreased AsA Content in Etiolated Seedlings.

(A) Comparison of the AsA content between light-grown and etiolated Col-0 and Ws seedlings. The AsA content of 1-week-old seedlings grown on Murashige and Skoog (MS) medium with (control) or without (etiolated) light was determined. The data are the mean values and SD of three replicates. FW, fresh weight.

(B) VTC1 protein abundance in light-grown (control) and etiolated Col-0 and Ws seedlings. Total protein extracts (10 μg) were used for immunoblotting with anti-VTC1 and anti-actin antibodies (as a loading control).

RESULTS

VTC1 Interacts with the CSN Subunit CSN5B in Yeast and Plants

To determine whether light/darkness affects AsA production and the protein levels of AsA biosynthetic enzymes, we first measured the AsA content in light-grown (50 μmol/m^2/s) and etiolated *Arabidopsis* seedlings of ecotypes Columbia-0 (Col-0) and Wassilewskija (Ws). Etiolated seedlings of both ecotypes contained 70% less AsA than light-grown seedlings (Figure 1A). We next measured the VTC1 protein level in etiolated seedlings of both ecotypes. The VTC1 protein levels in the etiolated seedlings were lower than in the light-grown seedlings (Figure 1B), indicating that the protein level of VTC1 is associated with the regulation of AsA synthesis in response to light/darkness.

To isolate light/darkness-related factors in AsA synthesis, a yeast two-hybrid screen was performed to identify VTC1-interacting proteins by screening a cDNA library prepared from 3-d-old etiolated *Arabidopsis* seedlings. Among the 15 cDNA clones recovered, seven were found to encode CSN5B. CSN5B reportedly belongs to a CSN complex containing eight subunits (CSN1 to CSN8; Wei and Deng, 2003). Several studies have suggested that the CSN, COP1-SPA, and CDD complexes (Constitutive photomorphogenesis10, DNA Damage-binding protein1, and De-etiolated1) negatively regulate photomorphogenesis in *Arabidopsis* via proteasomal degradation (Chen et al., 2010; Nezames and Deng, 2012). Curiously, all of the isolated CSN5B clones in our assays were partial clones that lacked the 17 N-terminal and 29 C-terminal amino acids. Because full-length CSN5 fused with the GAL4 activation domain (GAL4-AD) nonspecifically interacted with tested proteins in yeast, but N-terminally truncated CSN5 did not (Lozano-Durán et al., 2011), we fused truncated CSN5B, lacking the 17 N-terminal residues and 29 C-terminal amino acids, to the GAL4 DNA binding domain (GAL4-BD); this fusion interacted with VTC1-AD (Figure 2A), indicating that CSN5B interacts specifically with VTC1 in yeast. To further verify this interaction, we generated a series of VTC1 truncations that were fused with the GAL4-BD and used them in yeast two-hybrid assays. We found that CSN5B interacted with different VTC1 N-terminal truncations, all of which included the N-terminal 40 amino acids (N5, amino acids 1 to 200; N4, 1 to 160; N3, 1 to 120; N2, 1 to 80; and N1, 1 to 40). Interactions were not detected between CSN5B and the VTC1 C-terminal conserved domain bacterial transferase hexapeptide or between CSN5B and a VTC1 deletion lacking the N-terminal 40 amino acids (delet-N1) (Figure 2B), suggesting that the N-terminal 40 amino acid fragment of VTC1 is necessary for its interaction with CSN5B.

To identify the interaction between VTC1 and CSN5B in plants, we performed coimmunoprecipitation (CoIP) assays using an F1 hybrid of OE2/CSN5B-myc, which was generated by crossing a transgenic OE2 line that constitutively expressed the full-length *VTC1* cDNA-HA-epitope tag in Col-0 with a CSN5B-myc line overexpressing CSN5B-myc in Col-0. The α-myc matrix efficiently immunoprecipitated the CSN5B-myc fusion and VTC1-HA protein from extracts of OE2/CSN5B-myc plants but not from OE2 seedlings, which were used as a negative control (Figure 2C). The following three experiments also suggested that the N-terminal region of VTC1 interacts with the N-terminal region of CSN5B in plants: (1) CoIP assays using extracts of hybrids of the OE2 line or a transgenic line overexpressing the nucleotidyl transferase (NT) fragment from the N terminus of VTC1 with the CSN5B-myc line (Figure 2D); (2) pull-down experiments using purified CSN5B to isolate proteins from the OE2 line (Figure 2E); and (3) a bimolecular fluorescence

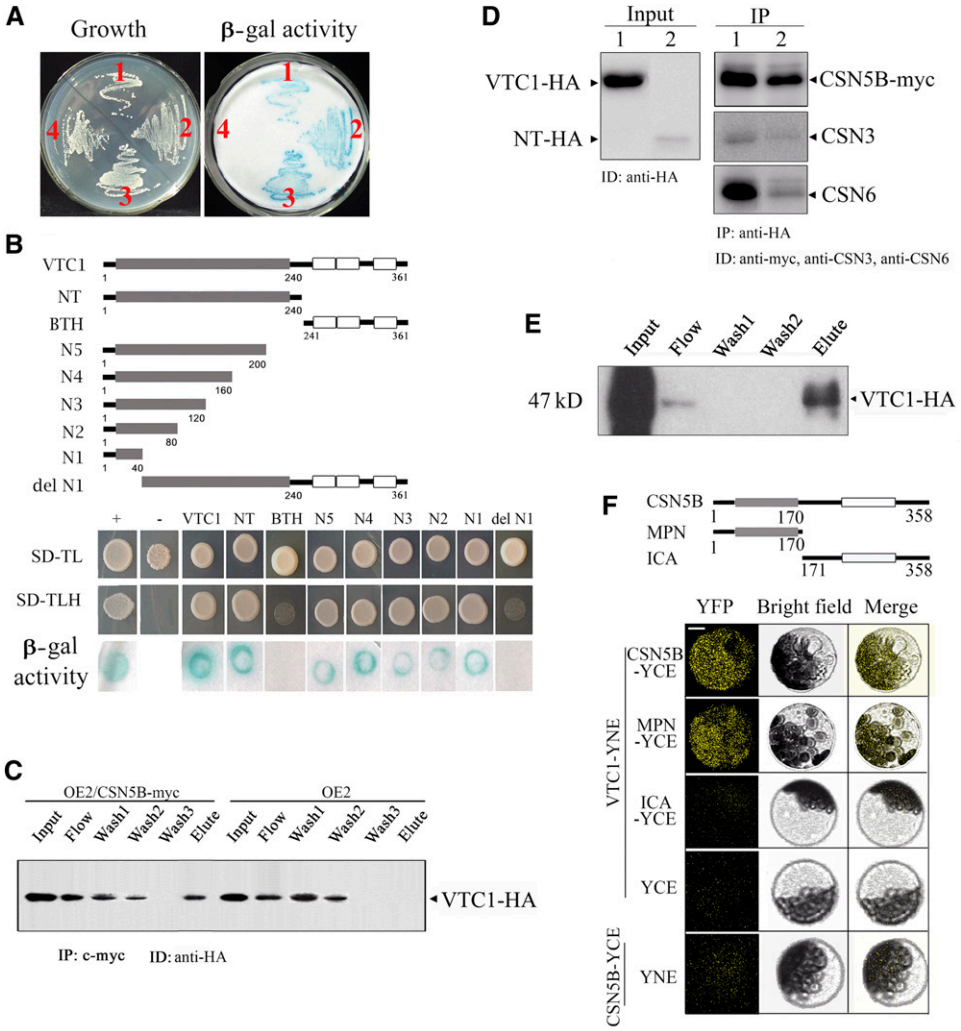

Figure 2. VTC1 Interacts with CSN5B in Yeast and Plants.

(A) VTC1 interacts with truncated CSN5B in a yeast two-hybrid assay. p53:T7 (Clontech) alone (positive control) (1), pAS1-CYH-VTC1 and pACT-CSN5B (2), pAS1-CYH-CSN5B and pACT-VTC1 (3), or pAS1-CYH-VTC1 and the empty prey pACT vector (4; negative control) were cotransformed into yeast cells. The full-length cDNA of *VTC1* and truncated *CSN5B* (amino acids 18 to 329) were used. The left panel shows the growth of the transformed yeast on SD/-Trp-Leu-His medium containing 15 mM 3-AT. The right panel shows a filter assay for β-galactosidase (β-gal) activity.

(B) The interaction between the truncated version of CSN5B (amino acids 18 to 329) and a series of VTC1 deletions in yeast. The top panel illustrates the following constructs: full-length *VTC1*, the conserved N-terminal NT and C-terminal bacterial transferase hexapeptide domains of VTC1, and different fragments of VTC1 (N1-5). The bottom panels show the growth of the transformed yeast cells on SD/-Trp-Leu (SD-TL) or SD/-Trp-Leu-His (SD-TLH) medium containing 15 mM 3-AT and a filter assay for β-galactosidase activity of the transformants grown on SD/-Trp-Leu-His. The yeast two-hybrid system is the same as shown in **(A)**.

(C) The interaction between VTC1 and full-length CSN5B in vivo. Immunoprecipitated samples were obtained from OE2 plants that overexpressed VTC1-HA and an F1 hybrid (OE2/CSN5B-myc) that was generated by crossing OE2 with the CSN5B-myc–overexpressing full-length *CSN5B* transgenic line. Total soluble protein extracts (Input) from OE2/CSN5B-myc or OE2 were incubated with a monoclonal α-myc 9E10 affinity matrix (see Methods). The flow-through was collected after centrifugation (Flow) and three washes (Wash1, Wash2, and Wash3). The immunoprecipitated (IP) proteins were eluted and separated by 12% SDS-PAGE for immunoblotting with anti-HA antibodies. ID, immunoblot detection.

(D) CoIP of CSN and full-length or the NT domain of VTC1. Total soluble protein extracts (Input) from the F1 hybrid cross of CSN5B-myc/OE2 (indicated as number 1) or CSN5B-myc/NT-HA/Col-0 overexpressing the NT domain of *VTC1* in Col-0 (indicated as number 2) were incubated with agarose fused to anti-HA mouse antibodies (see Methods). The eluted fractions were separated by 12% SDS-PAGE and immunoblotted with anti-myc (to detect myc-tagged CSN5B), anti-CSN3, and anti-CSN6 antibodies. The detected proteins are indicated by arrowheads.

(E) Pull-down assays for the interaction of VTC1 with CSN5B. Purified His-CSN5B was used to copurify VTC1-HA from OE2 seedling protein extracts (Input) following incubation with His-Select Nickel Affinity Gel (see Methods). The flow-through was collected after centrifugation (Flow) and two washes (Wash1 and Wash2), and the eluted fractions were separated by 12% SDS-PAGE and immunoblotted with anti-HA antibodies. The number on the left indicates the molecular mass of the HA-VTC1 fusion.

complementation (BiFC) assay using *Arabidopsis* protoplasts to detect the interaction of VTC1 with full-length and N-terminal (MPN), but not C-terminal (ICA), CSN5B (Figure 2F).

VTC1 Is Associated with the CSN Complex

CSN5 participates in important biological functions and harbors the catalytic center of CSN's derubylation activity, which can function independently of the CSN in vivo (Wei and Deng, 2003; Wei et al., 2008). Moreover, two CSN5 isoforms can be incorporated into distinct CSN complexes in vivo (CSN^{CSN5A} and CSN^{CSN5B}) in *Arabidopsis* (Gusmaroli et al., 2004). To test whether VTC1 interacts with other CSN subunits, we first used a yeast two-hybrid assay to screen for interacting proteins. VTC1 interacted with CSN5A and CSN5B but did not interact with other CSN subunits (Figure 3A). Interestingly, the VTC1–CSN5B interaction was much stronger than that of VTC1-CSN5A (Figure 3A), even though *CSN5B* was expressed at a lower level than *CSN5A* in both the dark and light (see Supplemental Figure 1 online). We also compared the interaction between VTC1 and CSN5A or CSN5B in vivo in CSN5A-myc or CSN5B-myc transgenic lines that expressed CSN5A-myc or CSN5B-myc, respectively, in a *csn5b* background. CSN5B, but not CSN5A, was coimmunoprecipitated with VTC1 (see Supplemental Figure 2 online), suggesting that VTC1 interacts specifically with CSN5B in plants.

We next found that the VTC1–CSN5B interaction is associated with the CSN holocomplex in plants based on a gel filtration profile using extracts of transgenic OE2 plants. Protein blot analyses indicated that the proteins that associated with VTC1-HA were eluted in high molecular mass fractions (Figure 3B), which may correspond to the CSN complex (fractions 12 to 15; Gusmaroli et al., 2007). To identify the CSN complex, we probed the gel filtration profile separately with antibodies against CSN3, CSN5, and CSN6. As expected, VTC1 cofractionated with CSN3, CSN5, and CSN6 (Figure 3B), consistent with the previous report that the CSN complex was centered between 450 and 550 kD (Kwok et al., 1998). The coelution of VTC1 and CSN from the gel filtration column indicates that they are part of the same complex. Because the CSN holocomplex is predominantly localized to the nucleus, and the D-Man/L-Gal pathway exists in the cytoplasm, we further investigated the localization of VTC1 by isolating nuclei and cytoplasm from OE2 seedlings. VTC1-HA was detected in both the nucleus and the cytoplasm (Figure 3C). Furthermore, CSN3 and CSN6 could be coimmunoprecipitated with VTC1-HA and NT-HA (similar to CSN5B-myc) (Figure 2D), strongly suggesting that the VTC1–CSN5B interaction is associated with the CSN complex.

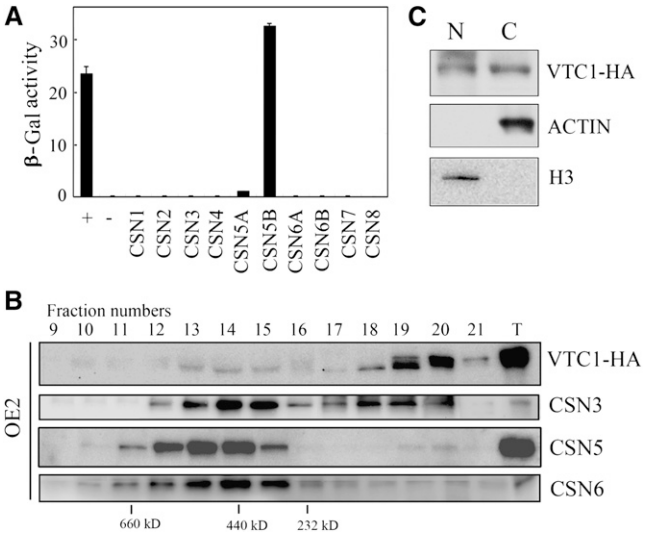

Figure 3. VTC1 Associates with the CSN Complex by Interacting with CSN5B.

(A) The interaction between VTC1 and the CSN complex in a yeast two-hybrid assay. VTC1 was used as bait, and CSN1, CSN2, CSN3, CSN4, CSN5A, CSN5B, CSN6A, CSN6B, CSN7, and CSN8 were used as the prey; the yeast two-hybrid system is the same as described in Figure 2A. The full-length cDNAs of the CSN genes (except CSN5B, amino acids 18 to 329) were used. β-Galactosidase (β-Gal) activity was detected. The value is the average of six individual yeast colonies, and the error bars represent the SD.

(B) The association of VTC1 with the CSN complex in a gel filtration assay. Total proteins (500 μg) extracted from 10-d-old OE2 seedlings grown under normal conditions were subjected to Superose 6 gel filtration chromatography. The column fractions were subjected to SDS-PAGE and immunoblot analyses with anti-HA, anti-CSN3, anti-CSN5, and anti-CSN6 polyclonal antibodies. The fraction numbers were labeled 9 to 21. T indicates the total unfractionated extract.

(C) Immunoblot analysis of the subcellular localization of VTC1 in the OE2 line. Total proteins were extracted from 10-d-old OE2 seedlings, and nuclear (N) and cytosolic (C) proteins were isolated with a plant nuclei isolation/extraction kit. VTC1 protein was detected with anti-HA antibodies. Antibodies against actin and histone H3 were used to identify the cytosolic and nuclear fractions, respectively.

CSN5B Promotes VTC1 Degradation under Dark Conditions through the 26S Proteasome Pathway

AsA content has been reported to decrease under dark conditions and during the transition from high light to low light (Dowdle et al., 2007). The CSN complex regulates photomorphogenesis by regulating cullin-RING E3 ubiquitin ligase

Figure 2. (continued).

(F) Analyses of BiFC to detect the interaction between VTC1 and CSN5B. The top panel shows the full-length, N-terminal MPN and C-terminal ICA of CSN5B. The N terminus of yellow fluorescent protein (YNE) was fused to full-length VTC1, and various CSN5B fragments were fused to the C terminus of yellow fluorescent protein (YCE). Combinations of the plasmids and controls (indicated on the left) were transformed into *Arabidopsis* protoplasts. The bottom panels indicate the presence of yellow fluorescent protein signal due to the reconstitution of yellow fluorescent protein through protein–protein interactions of the tested pairs. Bar = 10 μm.

degradation (Schwechheimer and Isono, 2010). We determined that etiolated seedlings displayed low levels of VTC1 protein (Figure 1B) and that CSN5B interacted with VTC1 in vivo (Figures 2C, 2D, and 2F). Based on these data, we asked whether darkness inhibits VTC1 protein stability, thereby mediating the effects of CSN5B. To address this, we measured the VTC1 protein levels in 10-d-old OE2 and OX4 seedlings, which constitutively expressed VTC1-HA in a Col-0 and *csn5b* background, respectively. Immunoblot analysis showed that the VTC1 protein levels decreased and then nearly disappeared after the seedlings were transferred to darkness for 8 and 12 h, respectively, compared with light-grown seedlings (Figure 4A). We also found that VTC1 was stabilized when OX4 seedlings were transferred to darkness for 12 h (Figure 4B). To further determine the effect of CSN5B on VTC1 stability, we expressed a VTC1-GFP (for green fluorescent protein) fusion in both the Col-0 and *csn5b* backgrounds. For each transformation, we selected the line in which *VTC1* expression was not obviously different at the transcriptional level. We detected VTC1 in extracts of etiolated seedlings using anti-GFP antibody and found that VTC1 was clearly accumulated in the *VTC1-GFP*–overexpressing line in a *csn5b* background compared with the *VTC1-GFP*–overexpressing line in Col-0 (see Supplemental Figure 3 online). These results suggest that CSN5B promotes VTC1 degradation in darkness.

To confirm whether VTC1 degradation is mediated by proteasomal degradation, we used an inhibitor of the 26S proteasome system to pretreat OE2 seedlings in the dark for 10 h. VTC1 protein accumulated to a greater degree in the MG132-pretreated samples than in the DMSO-pretreated samples (Figure 4C), indicating that the ability of CSN5B to promote VTC1 degradation may be mediated through the 26S proteasome system. Moreover, higher molecular mass forms of VTC1-HA were detected in extracts of etiolated seedlings from the OE2 transgenic line; this result was confirmed by detection with an antiubiquitin antibody (Figure 4D), suggesting that the VTC1-HA fusion was linked with polyubiquitin. Meanwhile, the gel filtration profile from extracts of transgenic OE2 plants was detected with the same ubiquitin antibody; our results showed that ubiquitin was present in the higher molecular mass fractions (see Supplemental Figure 4 online). Therefore, VTC1 may be ubiquitinated in vivo to promote its degradation via the 26S proteasome system in darkness.

CSN5B Is Required to Regulate AsA Synthesis in a Light-Dependent Manner

Because light is an important environmental signal for VTC1 protein stability and VTC1 degradation is dependent upon CSN5B regulation, we asked whether CSN5B functionally contributes to maintenance of the AsA level in plants. Therefore, we compared the AsA contents of Col-0, *csn5b*, *csn5a*, and the typical *cop* phenotype mutant *csn8*. Our analyses demonstrated that *csn5b*, but not *csn5a*, contained higher AsA levels than Col-0 (Figure 5, left panel), indicating that CSN5A and CSN5B contribute differentially to the regulation of the AsA content. It is also noteworthy that the AsA content in *csn8* was increased compared with that in Col-0 (Figure 5, left panel). To further

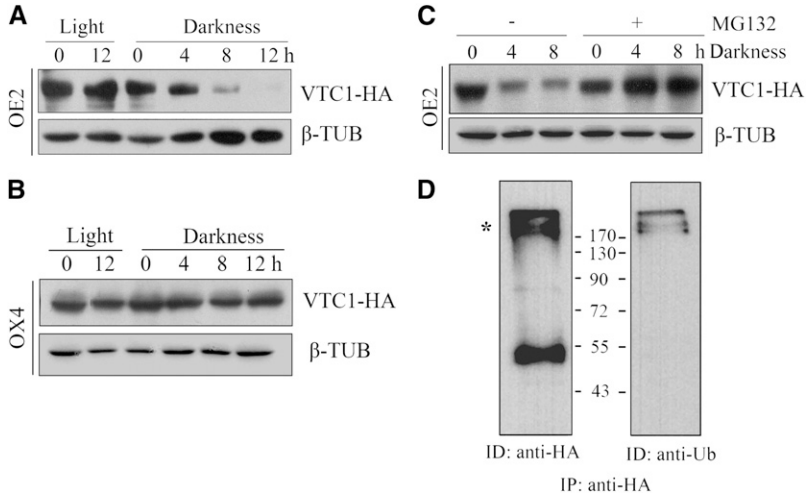

Figure 4. Under Darkness, CSN5B Promotes VTC1 Degradation through the 26S Proteasome Pathway.

(A) OE2 seedlings, overexpressing a VCT1-HA fusion in the Col-0 background, grown under normal conditions were transferred to liquid MS medium supplemented with 500 μM cycloheximide, followed by treatment with or without light (50 μmol/m^2/s) for the indicated time.

(B) OX4 seedlings, overexpressing a VTC1-HA fusion in the *csn5b* background, grown under normal conditions were transferred to liquid MS medium supplemented with 500 μM cycloheximide, followed by treatment with or without light for the indicated time.

(C) OE2 seedlings dark treated as in **(A)** were treated with the proteasome inhibitor MG132 (50 μM, +) or DMSO (control, −).

(D) Ubiquitination of VTC1 in the OE2 seedlings treated with 50 μM MG132. ID, immunoblot detection; IP, immunoprecipitation.

Total proteins were extracted from 10-d-old etiolated OE2 or OX4. Anti-HA or antiubiquitin antibodies were used to detect VTC1-HA and ubiquitinated VTC1-HA, respectively. An asterisk indicates the ubiquitinated form of VTC1. Antibodies against β-tubulin (β-TUB) were used as a loading control.

investigate the role of CSN5B in regulating the plant AsA content, we measured the AsA content of the double mutant *vtc1-1 csn5b*. As reported previously, the AsA level in *vtc1-1* was only 30% of that in Col-0, while that of the double mutant *vtc1-1 csn5b* was twofold higher than the level in *vtc1-1* but was lower than in *csn5b* (Figure 5, left panel). These results demonstrate that a loss of *CSN5B* function enhanced AsA content but could not fully restore the AsA deficit induced by the reduced activity of VTC1 in *vtc1-1*.

To define the effect of CSN5B on the light-regulated AsA content in plants, we measured the AsA contents of Col-0, *vtc1-1*, and *csn5b* seedlings that were exposed to continuous darkness or light. After 24 h of darkness, Col-0 and *vtc1-1* contained ~30% less AsA than before treatment, but the AsA content of *csn5b* was unaffected (Figure 5, middle panel). By contrast, Col-0 contained 30% more AsA following 24 h of continuous light compared with the control, but no AsA content changes were observed in *csn5b* (Figure 5, right panel), suggesting that the loss of *CSN5B* function impaired the effect of light/darkness on the plant AsA content.

A Loss of Function of CSN5B Enhances Salt Tolerance and Reduces the Oxidative Stress Response

Previous studies have demonstrated that AsA-deficient mutants are salt sensitive (Huang et al., 2005) and that the transcriptional regulator ERF98 enhances salt resistance by activating *VTC1* expression and AsA synthesis in *Arabidopsis* (Zhang et al., 2012). Therefore, we asked whether the regulation of VTC1 by CSN5B is responsible for salt stress tolerance. To address this, we transferred germinated seeds of various genotypes to Murashige and Skoog (MS) medium in the presence or absence of NaCl. No obvious differences were observed among the different genotypes under normal growth conditions. However, after exposure to 100 mM NaCl for 10 d, *vtc1-1 csb5b* and *vtc1-1* displayed clearly retarded seedling growth compared with Col-0, including shorter roots, smaller leaves with shorter petioles and slower leaf growth, while the *csn5b* seedlings displayed shorter petioles and longer roots (Figure 6A). It is not surprising that *vtc1-1* growth was severely inhibited due to its lower AsA content, whereas the double mutant *vtc1-1 csn5b* displayed better growth than *vtc1-1* due to its increased AsA level. Further analysis showed that the fresh weight and root length in the *vtc1-1 csb5b* and *vtc1-1* mutants were significantly less than those in Col-0, whereas the fresh weight and root elongation in the *csn5b* plants did not obviously change following salt treatment (Figure 6B). These results demonstrate that a loss of function of CSN5B enhances tolerance to salt.

AsA is an essential antioxidant in plants and animals and efficiently scavenges reactive oxygen species (ROS), including superoxide radicals and oxidative stress–generated hydrogen peroxide (Kärkönen and Fry, 2006; Ishikawa and Shigeoka, 2008; Barth et al., 2010). Methyl viologen (MV) can reportedly generate superoxide radicals (Bus and Gibson, 1984). Because *csn5b* plants contain increased AsA levels, we speculated that CSN5B affects the oxidative stress response. To address this hypothesis, we treated *csn5b* mutants with 50 μM MV for 24 h. Compared with Col-0 seedlings, *vtc1-1* was very sensitive to MV, whereas *csn5b* was insensitive to MV (see Supplemental Figure 5A online); these results are consistent with the environmental stress sensitivity of *vtc1-1* (Conklin et al., 1996). Accumulated ROS may damage cellular DNA, lipids, and proteins, and malondialdehyde (MDA) is an important product of lipid peroxidation (Tajdoost et al., 2007); therefore, we examined the MDA content in plants of various genotypes. Indeed, *vtc1-1* accumulated the most MDA, but the MDA content in *csn5b* was much lower than that in Col-0 following MV treatment, although no apparent differences were observed between Col-0 and *csn5b* plants under normal conditions (see Supplemental Figure 5B online). These results suggest that *csn5b* mutant plants show a reduced response to oxidative stress.

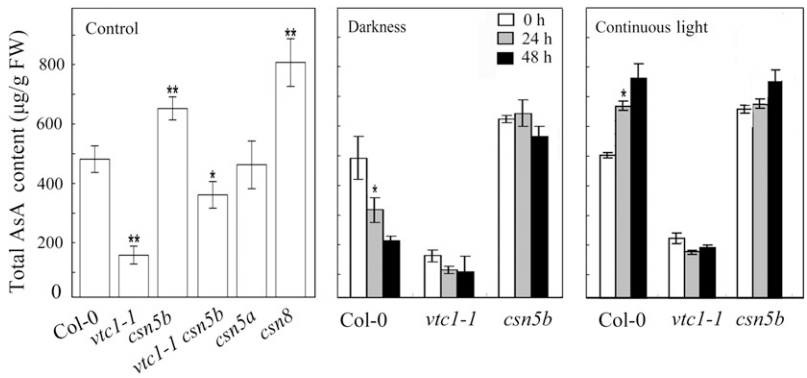

Figure 5. CSN5B Is Required for Regulation of the AsA Content by Light.

The total AsA content of 10-d-old Col-0, *vtc1-1*, *csn5*b, *vtc1-1 csn5b*, *csn5a*, and *csn8* seedlings under normal growth conditions (left panel) and the total AsA content of 10-d-old Col-0, *vtc1-1*, and *csn5b* seedlings grown under a 16-h-light/8-h-dark cycle followed by treatment with continuous dark (middle panel) or continuous light (right panel) for 24 or 48 h. The mean values and SD of three replicates are shown. Asterisks indicate a significant difference as determined using Student's *t* test compared with Col-0 in the left panel and compared with 0 h of treatment in the middle and right panels (*$P < 0.05$; **$P < 0.01$). FW, fresh weight.

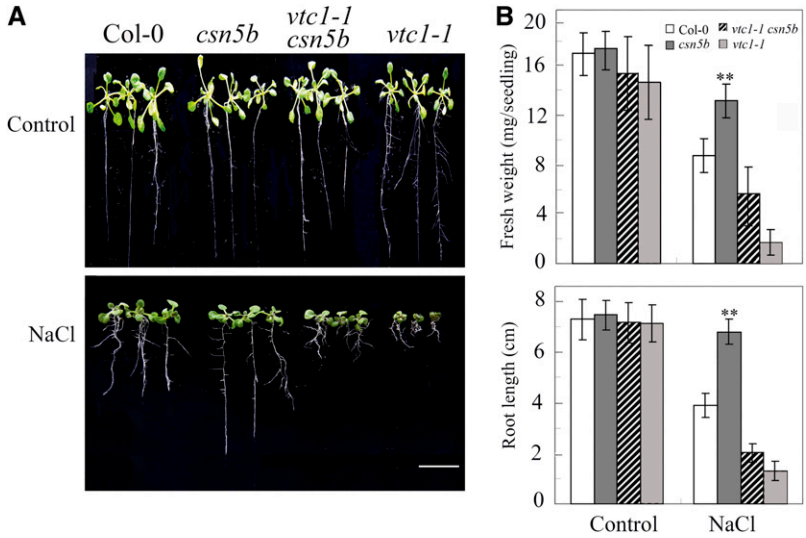

Figure 6. The *csn5b* Mutant Is Insensitive to NaCl.

(A) Phenotype of 10-d-old seedlings exposed to salt. Germinated seeds of Col-0, *csn5b*, *vtc1-1 csn5b*, and *vtc1-1* were planted on MS medium supplemented with or without NaCl, and the seedlings were photographed after 10 d. Bar = 2 cm.

(B) Fresh weight of Col-0, *csn5b*, *vtc1-1 csn5b*, and *vtc1-1* seedlings after NaCl treatment as in **(A)**. The data were obtained from an average of 20 seedlings in triplicate. The error bars indicate the SD. P values (versus Col-0 after salt induction) were determined using a two-tailed Student's *t* test assuming equal variance (*P < 0.05; **P < 0.01).

DISCUSSION

It is well known that light plays an important role in plant development and contributes to the determination of AsA levels (Yabuta et al., 2007). Recently, several regulators of AsA biosynthesis in plants have been shown to modulate the transcription of AsA synthesis genes (Zhang et al., 2009, 2012). This investigation shows that the photomorphogenic factor CSN5B links light modulation with AsA synthesis at the posttranslational level. First, VTC1 was more stable in light than in dark conditions. VTC1 was found to be polyubiquitinated and degraded in darkness; however, this degradation was inhibited by the 26S proteasome inhibitor MG132. Second, as a subunit of the light-related regulator CSN, CSN5B interacted with VTC1 and promoted its degradation, indicating that CSN5B is a posttranslational regulator of AsA synthesis. Third, a loss of *CSN5B* function impaired the effect of light on AsA synthesis in response to continuous light or darkness.

The CSN complex regulates the activity of cullin-RING E3 ubiquitin ligases (Dohmann et al., 2005; Chen et al., 2010; Schwechheimer and Isono, 2010). Studies have also indicated that the CSN5 subunit harbors the activity center of the CSN, resulting in the degradation via nuclear export of its binding targets in mammalian cells (Wei et al., 2008). Among the eight CSN subunits, CSN5 can bind numerous regulators and differentially affects the stability of each; the multiple functions of CSN5 have been extensively explored in mammalian cells (Liu et al., 2009). The null mutant *csn5a* phenotype is less severe than the lethal *fusca* phenotype of the *csn5a csn5b* double null mutant, suggesting that CSN5A is the predominantly functional subunit, whereas the contribution of CSN5B to CSN5 is unclear (Gusmaroli et al., 2004). In this report, we found that CSN5B functions in *Arabidopsis* as a regulator of AsA synthesis and is associated with the CSN complex through its physical interaction with VTC1. Because CSN5A and CSN5B share high sequence similarity, it is not surprising that VTC1 can interact with CSN5A in yeast. However, even though *CSN5A* is expressed at a higher level than *CSN5B*, CSN5A does not interact with VTC1 in vivo. Importantly, the evidence presented here that the N-terminal conserved MPN domain of CSN5B interacted with VTC1 further indicates that the conserved N termini of CSN5A and CSN5B are key domains that distinguish their regulation of plant growth and development. Therefore, it is important to identify the key amino acids within the MPN domains of CSN5A and CSN5B. Although the antibodies against CSN5 recognize both CSN5A and CSN5B isoforms, because of the specific interaction of VTC1 with CSN5B in plants, the detection of CSN5 in gel filtration chromatography fractions from OE2 seedlings further indicates that VTC1, CSN3, CSN5B, and CSN6 are from the same complex. In addition, a loss of CSN5A or CSN5B function revealed that the two proteins play unequal roles in affecting AsA levels in seedlings. The *csn5b* seedlings contained higher AsA levels, and the regulation of VTC1 by CSN5B occurs through the CSN complex. Notably, the *csn8* mutant has a high AsA content, although CSN8 does not interact with VTC1 in yeast. Thus, CSN8 may be involved in modulating VTC1 stability or AsA biosynthesis, and the CSN complex may have an additional function in AsA biosynthesis. Together, these results strongly suggest that the CSN^{CSN5B} complex, whose role in photomorphogenesis is unknown (Gusmaroli et al., 2004), plays a role in modulating AsA biosynthesis in plants.

Several studies have indicated that ubiquitination is frequently used as a posttranslational mechanism to modulate the stability, intracellular localization, and function of proteins in response to environmental signals in eukaryotic cells (Gao and Karin, 2005; Miranda and Sorkin, 2007). Some components of the light-related signaling pathways underlying photomorphogenesis, the circadian clock, and photoperiodic flowering are first ubiquitinated and subsequently degraded by the 26S proteasome in the dark (Saijo et al., 2003; Seo et al., 2003; Yang et al., 2005; Datta et al., 2006; Jang et al., 2008). The CSN holocomplex regulates protein turnover through the 26S proteasome (Nezames and Deng, 2012), and the CSN also plays a major role in circadian function in *Neurospora* (Zhou et al., 2012). The evidence presented in this study that VTC1 can be ubiquitinated and degraded via the 26S proteasome in the dark supports previous findings showing that the total AsA leaf content is light dependent and controlled by the circadian clock (Dowdle et al., 2007). Moreover, CSN5B negatively regulates AsA synthesis by regulating VTC1 stability through the interaction between the N-terminal 40–amino acid fragment of VTC1 and the N-terminal conserved MPN domain of CSN5B. The AsA-deficient mutant *vtc1-1* has been reported to contain 30% less AsA than wild-type plants because of its P22S mutation; this mutation affects VTC1 enzymatic activity and stability but not transcription or mRNA stability (Conklin et al., 1999), indicating that the amino acids around VTC1 P22 may play important roles in the modulation of VTC1 protein stability. To further determine how this regulation occurs, we analyzed the VTC1 N-terminal amino acid sequences from different species. Our alignment revealed that the N-terminal 40–amino acid motif of VTC1 was conserved with the exception of P22, D27, and A29 (see Supplemental Figure 6 online). This study demonstrates that the amino acid at position 27 affects the interaction with CSN5B, indicating that CSN5B modulates VTC1 by interacting with the amino acids surrounding VTC1 P22, which affects VTC1 protein stability. Therefore, it will be vital to investigate how these key amino acids affect the interaction with CSN5B or the activity of VTC1 in plants.

Accumulating data indicate that increased AsA content could enhance tolerance to salt stress in plants (Hemavathi et al., 2010; Zhang et al., 2012); indeed, an AsA-deficient mutant showed sensitivity to salt stress (Huang et al., 2005). Therefore, it is reasonable that the higher AsA content in *csn5b* confers tolerance to salt stress. Alternatively, given evidence showing that *vtc1-1* is hypersensitive to ammonium and that VTC1 has functions in cell wall polysaccharide synthesis and protein *N*-glycosylation (Qin et al., 2008; Barth et al., 2010), it is possible that the modulation of CSN5B by VTC1 results in altered glycoprotein synthesis, which further affects the *csn5b* response to salt stress. In addition, one important role of AsA is to remove ROS, which are triggered by light and oxidative stress, in plants (Smirnoff, 2000; Li et al., 2010). Plants require many small molecules to maintain a steady redox state in vivo. Under oxidative stress, seedlings need more AsA to eliminate ROS (Smirnoff and Pallanca, 1996). Because ROS are produced under conditions of oxidative or salt stress in the light and these ROS must be removed in a timely manner due to their toxicity, VTC1 stability in the light promotes AsA biosynthesis, providing a reducing agent. By contrast, in the dark, CSN5B promotes VTC1 degradation via the 26S proteasome pathway to maintain a lower AsA content.

Based on this research and previous studies, we propose that in the light VTC1 exists in a free form or as part of the CSN in cytoplasts and that stable VTC1 protein promotes AsA or glycoprotein synthesis to maintain growth and prevent ROS-related damage. In the dark, VTC1 could enter the nucleus with the CSN through its interaction with CSN5B and subsequently be degraded by the 26S proteasome, resulting in lower AsA content. Whether other enzymes involved in AsA biosynthesis are modulated by the CSN remains to be discovered. Future efforts to identify VTC1-interacting E3 ligases and other light regulators of AsA levels will contribute to the determination of the mechanism by which AsA biosynthesis is modulated.

METHODS

Plant Materials and Growth Conditions

Wild-type *Arabidopsis thaliana* plants (ecotypes Col-0 and Ws) were used in this study. The AsA-deficient mutant *vtc1-1* (Conklin et al., 1996) was obtained from the ABRC. The cop mutants *csn5b*, *csn5a*, and *csn8* (*cop9-1*) and the CSN5B-myc– and CSN5A-myc–overexpressing transgenic lines are described elsewhere (Gusmaroli et al., 2004). The *vtc1-1 csn5b* double mutant was generated by crossing *vtc1-1* with *csn5b*; the homozygous double mutant was identified by sequencing *vtc1-1* and amplifying the *csn5b* T-DNA insertion using the primers listed in Supplemental Table 1 online. Full-length or N-terminal NT cDNA of *VTC1* was amplified by PCR using specific primers (see Supplemental Table 1 online) and cloned in frame with an HA or GFP tag into pCAMBIA1307 (a derivative of pCAMBIA1300 carrying the 2*cauliflower mosaic virus 35S promoter and the Octopine synthase [OCS] terminator). The resulting plasmids were then separately introduced into Col-0 and *csn5b*, respectively, using *Agrobacterium tumefaciens*–mediated transformation. The transgenic lines were selected with hygromycin and confirmed by PCR amplification. Approximately four to nine homozygous single-insertion lines were obtained for each transformation by analyzing the segregation ratio of T2 seeds grown on hygromycin. Transgenic plants overexpressing *VTC1-HA* in the Col-0 and *csn5b* backgrounds were named OE and OX, respectively, and the transgenic lines overexpressing *NT* in Col-0 or overexpressing *VTC1-GFP* in Col-0 and *csn5b* were named NT-HA, VTC1/Col-0, and VTC1/*csn5b*, respectively. The number that follows OE or OX indicates the transgenic line; lines OE2 and OX4, which displayed similar transcriptional levels, were used in this study. The CSN5B-myc transgenic lines were crossed with OE2 and NT-HA to produce F1 hybrids that were used for CoIP.

Arabidopsis seeds were surface sterilized and plated on solid MS medium containing 3% Suc. After ~3 to 4 d of cold (4°C) treatment, the plates were stored in a 22°C incubator for propagation. The seedlings were transferred from the plates to a 1:1 mixture of soil and vermiculite and grown to maturity at 22°C under a 16-h-light/8-h-dark cycle in a growth chamber. The light intensity was 50 μmol/m^2/s and the humidity was 70%.

Yeast Two-Hybrid Assays

To screen for interacting proteins, full-length *VTC1* cDNA was cloned into pAS1-CYH2 as bait and transformed into yeast strain Y190 using the lithium acetate method. The cDNA library from 3-d-old etiolated *Arabidopsis* seedlings was obtained from the ABRC (CD4-22), and library plasmids (20 μg) fused to pACT were transformed into yeast strain Y190 carrying the VTC1 bait (Kim et al., 1997). The entire transformation mixture

was plated onto a minimal agar base containing a -Trp-Leu-His dropout supplement (SD-Trp-Leu-His) (Clontech) and 15 mM 3-amino-1,2,4-triazole (3-AT) (Sigma-Aldrich). After screening for β-galactosidase activity (Breeden and Nasmyth, 1985), plasmid DNA was recovered from the yeast transformants using a TIANprep yeast plasmid DNA kit (Tiangen) and then transformed into *Escherichia coli* for sequencing.

To confirm the interaction, full-length and various *VTC1* cDNA fragments were cloned into pAS1-CYH2 as bait, and truncated CSN5B was cloned into pACT as prey. The two plasmids were then cotransformed into yeast strain Y190 according to the previously described procedure. The specific primers used to amplify each fragment and gene are listed in Supplemental Table 1 online. After growth on SD/-Trp-Leu or SD/-Trp-Leu-His medium, a filter assay was performed to test for β-galactosidase activity (Breeden and Nasmyth, 1985).

CoIP Analyses

For the in vivo CoIP analysis, *Arabidopsis* tissues were homogenized in immunoprecipitation buffer (Gusmaroli et al., 2004) containing 50 mM Tris-HCl, pH 7.5, 500 mM NaCl, 5 mM EDTA, 5% glycerol, 0.1% Nonidet P-40, 1 mM phenylmethylsulfonyl fluoride (PMSF) (Sigma-Aldrich) and 1× Complete protease inhibitor cocktail (Sigma-Aldrich). After centrifugation, the supernatants were filtered through 0.2-μm filters (Whatman), and the protein concentration was determined using the bicinchoninic acid (CWBIO) protein assay. Total protein (1 mg) was incubated with 30 μL of monoclonal α-myc 9E10 immobilized onto Sepharose Fast Flow beads (9E10 affinity matrix; Covance) or 30 μL of anti-HA-tag mouse antibody agarose (A2095; Sigma-Aldrich) overnight at 4°C on a rotary shaker. The matrix beads were washed three times with immunoprecipitation buffer and twice with 20 mM Tris-HCl, pH 7.5, 150 mM NaCl, and 5% glycerol. All of the wash steps were performed at 4°C for 10 min on a rotary shaker followed by centrifugation at 1500 rpm. The immunoprecipitated proteins were subsequently released by boiling in 5× SDS sample buffer and subjected to 12% SDS-PAGE. Immunoblot analyses using anti-HA and anti-myc antibodies (CWBIO) were then performed.

For the in vivo pull-down analysis, pET30a-CSN5B was transformed into bacterial cells to produce recombinant His-CSN5B. The recombinant protein was purified using His-Select Nickel Affinity Gel (Sigma-Aldrich) according to the manufacturer's instructions. Total plant proteins (1 mg) of OE2 were incubated with 10 μg of purified His-CSN5B protein bound to nickel affinity gel overnight at 4°C on a rotary shaker.

BiFC Assays

Full-length *VTC1* and *CSN5B* were cloned into the BiFC vector containing either the N- or C-terminal fragment of yellow fluorescent protein (pSPYNE-35S/pUC-SPYNE and pSPYCE-35S/pUC-SPYCE) (Walter et al., 2004), respectively. The primers used are listed in Supplemental Table 1 online. Plasmid DNA was extracted using a TIANprep Midi plasmid kit (Tiangen). The extraction and transfection of the protoplasts and microscopy were performed as described previously (Yoo et al., 2007).

Gel Filtration Chromatography

Arabidopsis tissues were homogenized in lysate buffer containing 20 mM Bis-Tris, pH 7.0, 500 mM ε-aminocaproic acid, 20 mM NaCl, 2 mM EDTA, 10% glycerol, freshly made 1 mM PMSF, 1× Complete protease inhibitor cocktail, 50 mM Na_3VO_4, and 10 mM NaF. Gel filtration chromatography was performed as described previously (Gusmaroli et al., 2004) except that the column was equilibrated with PBS containing 140 mM NaCl, 2.7 mM KCl, 10 mM Na_2HPO_4, and 1.8 mM KH_2PO_4. For the immunoblot analysis, fractions 9 to 21 were concentrated using acetone precipitation. Equal volumes of each fraction were loaded and detected with an anti-HA antibody and antibodies against the CSN subunits α-CSN3, α-CSN5, and α-CSN6 described previously (Gusmaroli et al., 2004).

Isolation of Nuclei

Nuclei were enriched using a plant nuclei isolation/extraction kit (Sigma-Aldrich) from 10 g of seedlings that were grown for 10 d on MS medium. Nuclei were isolated following the manufacturer's instructions. After the addition of Triton X-100, the supernatant was used as the cytosolic protein component. Antibodies against actin (CWBIO) and histone H3 (Sigma-Aldrich) were used to verify the cytosolic and nuclear fractions, respectively.

Detection of VTC1 Protein

For the in vivo protein degradation analysis, 10-d-old seedlings grown on MS plates were transferred to liquid MS medium and grown for an additional 8 h. The seedlings were then incubated in liquid MS medium containing 500 μM cycloheximide (Sigma-Aldrich) (Liu and Stone, 2010) with or without light (50 μmol/m^2/s). For proteasome inhibition, 50 μM MG132 (Sigma-Aldrich) was added; DMSO (the solvent for MG132, 0.2%) was used as a negative control. Following incubation, the seedlings were thoroughly washed with liquid MS medium three times to remove any residual DMSO or MG132. Total RNAs and proteins were then extracted separately. Antibodies against actin or β-tubulin (CWBIO) were used to examine the protein loading levels. Anti-VTC1 antibodies were generated by injecting *E. coli*–expressed recombinant VTC1 into rabbits (Youke).

In Vivo Ubiquitination Assay

Total proteins from 10-d-old OE2 seedlings were extracted with buffer containing 50 mM Tris-HCl, pH 7.5, 150 mM NaCl, 0.1% Nonidet P-40, 4 M urea, and 1 mM PMSF as described previously (Liu et al., 2010). The proteins (1 mg) were filtered and immunoprecipitated with agarose conjugated to anti-HA–tagged mouse antibodies for 4 h at room temperature as described above for CoIP; 50 μM MG132 was also added. The immunoprecipitation product was subjected to immunoblotting with anti-HA and antiubiquitin antibodies separately. The antiubiquitin monoclonal antibody has been described previously (Liu et al., 2010).

AsA Level Measurements

To measure the AsA levels, seedlings were grown on MS medium for 10 d. Approximately 0.1 g fresh weight of each sample was harvested and immediately ground in liquid nitrogen with a mortar and pestle. A quantitative analysis of AsA was performed by HPLC using nicotinic acid as an internal standard as described previously (Lykkesfeldt et al., 1995). The clear extracts (20 μL) were injected directly into the HPLC instrument (Shimadzu LC-10A), and chromatographic separation was achieved on an Agilent TC-C18 (250 × 4.6 mm, 5 μm) column and detected at 254 nm with an SPD M10A detector. Potassium dihydrogen phosphate (0.2 M) was used as the mobile phase; the pH was adjusted to 2.4 with phosphoric acid. AsA exists in oxidized and reduced forms in vivo. These different forms were transformed using AsA oxidase and DTT, respectively, and the difference in AsA peaks after oxidation reduction was used to determine the oxidized and reduced AsA contents, which together constituted the total AsA content.

RNA Extraction and Quantitative RT-PCR

Two micrograms of total RNA from each genotype was used to synthesize first-strand cDNA by RT reaction, then the products were used as

template for PCR or quantitative real-time PCR amplifications according to the manufacturer's instructions (Bio-Rad iQ5), as previously described (Zhang et al., 2012). Twenty-five RT-PCR amplification cycles were performed for *VTC1* and the internal control *Tublin4*. *CSN5A* and *CSN5B* expression levels were normalized to the expression level of the internal control *Tublin4* in the quantitative PCR experiment. The primers used are listed in Supplemental Table 1 online.

Assessment of Salt Tolerance and Measurement of the MDA Contents

For the salt tolerance assay, germinated seeds were cultured on MS medium with or without the addition of 100 mM NaCl for 10 d under normal growth conditions (22°C, 16-h-white light/8-h-dark cycle, 50 μmol/m^2/s).

To induce oxidative stress, 4-week-old seedlings were treated with 50 μM MV for 24 h. Detection of MDA contents was performed as described previously (Zhang et al., 2012).

Accession Numbers

The Arabidopsis Genome Initiative locus identifiers for the genes mentioned in this article are as follows: *VTC1* (At2g39770), *CSN5B* (At1g71230), *CSN5A* (At1g22920), *CSN1* (At3g61140), *CSN2* (At2g26990), *CSN3* (At5g14250), *CSN4* (At5g42970), *CSN6A* (At5g56280), *CSN6B* (At4g26430), *CSN7* (At1g02090), and *CSN8* (At4g14110). The germplasm numbers are as follows: *csn5b* (SALK_007134) and *csn5a* (SALK_063436).

Supplemental Data

The following materials are available in the online version of this article.

Supplemental Figure 1. *CSN5A* Shows Higher Transcript Levels Than *CSN5B*.

Supplemental Figure 2. CSN5A Does Not Interact with VTC1 in Vivo.

Supplemental Figure 3. CSN5B Promotes VTC1 Degradation in Plants.

Supplemental Figure 4. Ubiquitinated VTC1 Is Associated with the CSN Complex.

Supplemental Figure 5. The Mutant *csn5b* Exhibits Enhanced Tolerance to Oxidative Stress.

Supplemental Figure 6. Alignment of the VTC1 N-Terminal Amino Acid Sequences of Different Species.

Supplemental Table 1. List of the Primers Used in This Study.

ACKNOWLEDGMENTS

We thank Qi Xie (Institute of Genetics and Developmental Biology, Chinese Academy of Sciences) for providing the ubiquitin antibody. This work was supported by the National Basic Research Program of China (2012CB114204 and 2013CB127003) and the National Science Foundation of China (90917018 and 31171171).

AUTHOR CONTRIBUTIONS

R.H., X.W.D., and J.W. designed the research. J.W. and Y.Y. performed the research. L.M., R.H., J.W., Z.Z., R.Q., and H.Z. analyzed and discussed the data. R.H, X.W.D., and J.W. wrote the article.

Received November 1, 2012; revised January 3, 2013; accepted February 1, 2013; published February 19, 2013.

REFERENCES

Barth, C., Gouzd, Z.A., Steele, H.P., and Imperio, R.M. (2010). A mutation in GDP-mannose pyrophosphorylase causes conditional hypersensitivity to ammonium, resulting in *Arabidopsis* root growth inhibition, altered ammonium metabolism, and hormone homeostasis. J. Exp. Bot. **61:** 379–394.

Breeden, L., and Nasmyth, K. (1985). Regulation of the yeast *HO* gene. Cold Spring Harb. Symp. Quant. Biol. **50:** 643–650.

Bus, J.S., and Gibson, J.E. (1984). Paraquat: Model for oxidant-initiated toxicity. Environ. Health Perspect. **55:** 37–46.

Chen, H., Huang, X., Gusmaroli, G., Terzaghi, W., Lau, O.S., Yanagawa, Y., Zhang, Y., Li, J., Lee, J.H., Zhu, D., and Deng, X.W. (2010). *Arabidopsis* CULLIN4-damaged DNA binding protein 1 interacts with CONSTITUTIVELY PHOTOMORPHOGENIC1-SUPPRESSOR OF PHYA complexes to regulate photomorphogenesis and flowering time. Plant Cell **22:** 108–123.

Conklin, P.L., Norris, S.R., Wheeler, G.L., Williams, E.H., Smirnoff, N., and Last, R.L. (1999). Genetic evidence for the role of GDP-mannose in plant ascorbic acid (vitamin C) biosynthesis. Proc. Natl. Acad. Sci. USA **96:** 4198–4203.

Conklin, P.L., Williams, E.H., and Last, R.L. (1996). Environmental stress sensitivity of an ascorbic acid-deficient *Arabidopsis* mutant. Proc. Natl. Acad. Sci. USA **93:** 9970–9974.

Datta, S., Hettiarachchi, G.H., Deng, X.W., and Holm, M. (2006). *Arabidopsis* CONSTANS-LIKE3 is a positive regulator of red light signaling and root growth. Plant Cell **18:** 70–84.

Davey, M.W., Gilot, C., Persiau, G., Ostergaard, J., Han, Y., Bauw, G.C., and Van Montagu, M.C. (1999). Ascorbate biosynthesis in *Arabidopsis* cell suspension culture. Plant Physiol. **121:** 535–543.

Dohmann, E.M., Kuhnle, C., and Schwechheimer, C. (2005). Loss of the CONSTITUTIVE PHOTOMORPHOGENIC9 signalosome subunit 5 is sufficient to cause the cop/det/fus mutant phenotype in *Arabidopsis*. Plant Cell **17:** 1967–1978.

Dowdle, J., Ishikawa, T., Gatzek, S., Rolinski, S., and Smirnoff, N. (2007). Two genes in *Arabidopsis thaliana* encoding GDP-L-galactose phosphorylase are required for ascorbate biosynthesis and seedling viability. Plant J. **52:** 673–689.

Fukunaga, K., Fujikawa, Y., and Esaka, M. (2010). Light regulation of ascorbic acid biosynthesis in rice via light responsive *cis*-elements in genes encoding ascorbic acid biosynthetic enzymes. Biosci. Biotechnol. Biochem. **74:** 888–891.

Gao, M., and Karin, M. (2005). Regulating the regulators: Control of protein ubiquitination and ubiquitin-like modifications by extracellular stimuli. Mol. Cell **19:** 581–593.

Gatzek, S., Wheeler, G.L., and Smirnoff, N. (2002). Antisense suppression of l-galactose dehydrogenase in *Arabidopsis thaliana* provides evidence for its role in ascorbate synthesis and reveals light modulated l-galactose synthesis. Plant J. **30:** 541–553.

Gusmaroli, G., Feng, S., and Deng, X.W. (2004). The *Arabidopsis* CSN5A and CSN5B subunits are present in distinct COP9 signalosome complexes, and mutations in their JAMM domains exhibit differential dominant negative effects on development. Plant Cell **16:** 2984–3001.

Gusmaroli, G., Figueroa, P., Serino, G., and Deng, X.W. (2007). Role of the MPN subunits in COP9 signalosome assembly and activity, and their regulatory interaction with *Arabidopsis* Cullin3-based E3 ligases. Plant Cell **19:** 564–581.

Hemavathi, U., Upadhyaya, C.P., Akula, N., Young, K.E., Chun, S.C., Kim, D.H., and Park, S.W. (2010). Enhanced ascorbic acid accumulation in transgenic potato confers tolerance to various abiotic stresses. Biotechnol. Lett. **32:** 321–330.

Huang, C., He, W., Guo, J., Chang, X., Su, P., and Zhang, L. (2005). Increased sensitivity to salt stress in an ascorbate-deficient *Arabidopsis* mutant. J. Exp. Bot. **56:** 3041–3049.

Imai, T., Karita, S., Shiratori, G., Hattori, M., Nunome, T., Oba, K., and Hirai, M. (1998). L-galactono-gamma-lactone dehydrogenase from sweet potato: purification and cDNA sequence analysis. Plant Cell Physiol. **39:** 1350–1358.

Ioannidi, E., Kalamaki, M.S., Engineer, C., Pateraki, I., Alexandrou, D., Mellidou, I., Giovannonni, J., and Kanellis, A.K. (2009). Expression profiling of ascorbic acid-related genes during tomato fruit development and ripening and in response to stress conditions. J. Exp. Bot. **60:** 663–678.

Ishikawa, T., and Shigeoka, S. (2008). Recent advances in ascorbate biosynthesis and the physiological significance of ascorbate peroxidase in photosynthesizing organisms. Biosci. Biotechnol. Biochem. **72:** 1143–1154.

Jang, S., Marchal, V., Panigrahi, K.C., Wenkel, S., Soppe, W., Deng, X.W., Valverde, F., and Coupland, G. (2008). *Arabidopsis* COP1 shapes the temporal pattern of CO accumulation conferring a photoperiodic flowering response. EMBO J. **27:** 1277–1288.

Kärkönen, A., and Fry, S.C. (2006). Effect of ascorbate and its oxidation products on H_2O_2 production in cell-suspension cultures of *Picea abies* and in the absence of cells. J. Exp. Bot. **57:** 1633–1644.

Kim, J., Harter, K., and Theologis, A. (1997). Protein-protein interactions among the Aux/IAA proteins. Proc. Natl. Acad. Sci. USA **94:** 11786–11791.

Kwok, S.F., Solano, R., Tsuge, T., Chamovitz, D.A., Ecker, J.R., Matsui, M., and Deng, X.W. (1998). *Arabidopsis* homologs of a c-Jun coactivator are present both in monomeric form and in the COP9 complex, and their abundance is differentially affected by the pleiotropic cop/det/fus mutations. Plant Cell **10:** 1779–1790.

Laing, W.A., Bulley, S., Wright, M., Cooney, J., Jensen, D., Barraclough, D., and MacRae, E. (2004). A highly specific L-galactose-1-phosphate phosphatase on the path to ascorbate biosynthesis. Proc. Natl. Acad. Sci. USA **101:** 16976–16981.

Laing, W.A., Wright, M.A., Cooney, J., and Bulley, S.M. (2007). The missing step of the L-galactose pathway of ascorbate biosynthesis in plants, an L-galactose guanyltransferase, increases leaf ascorbate content. Proc. Natl. Acad. Sci. USA **104:** 9534–9539.

Li, F., Wu, Q.Y., Sun, Y.L., Wang, L.Y., Yang, X.H., and Meng, Q.W. (2010). Overexpression of chloroplastic monodehydroascorbate reductase enhanced tolerance to temperature and methyl viologen-mediated oxidative stresses. Physiol. Plant. **139:** 421–434.

Liu, H., and Stone, S.L. (2010). Abscisic acid increases *Arabidopsis* ABI5 transcription factor levels by promoting KEG E3 ligase self-ubiquitination and proteasomal degradation. Plant Cell **22:** 2630–2641.

Liu, L., Zhang, Y., Tang, S., Zhao, Q., Zhang, Z., Zhang, H., Dong, L., Guo, H., and Xie, Q. (2010). An efficient system to detect protein ubiquitination by agroinfiltration in *Nicotiana benthamiana*. Plant J. **61:** 893–903.

Liu, Y., Shah, S.V., Xiang, X., Wang, J., Deng, Z.B., Liu, C., Zhang, L., Wu, J., Edmonds, T., Jambor, C., Kappes, J.C., and Zhang, H.G. (2009). COP9-associated CSN5 regulates exosomal protein deubiquitination and sorting. Am. J. Pathol. **174:** 1415–1425.

Loewus, F.A. (1999). Biosynthesis and metabolism of ascorbic acid in plants and of analogs of ascorbic acid in fungi. Phytochemistry **52:** 193–210.

Lorence, A., Chevone, B.I., Mendes, P., and Nessler, C.L. (2004). *myo*-inositol oxygenase offers a possible entry point into plant ascorbate biosynthesis. Plant Physiol. **134:** 1200–1205.

Lozano-Durán, R., Rosas-Díaz, T., Gusmaroli, G., Luna, A.P., Taconnat, L., Deng, X.W., and Bejarano, E.R. (2011). Geminiviruses subvert ubiquitination by altering CSN-mediated derubylation of SCF E3 ligase complexes and inhibit jasmonate signaling in *Arabidopsis thaliana*. Plant Cell **23:** 1014–1032.

Lykkesfeldt, J., Loft, S., and Poulsen, H.E. (1995). Determination of ascorbic acid and dehydroascorbic acid in plasma by high-performance liquid chromatography with coulometric detection—Are they reliable biomarkers of oxidative stress? Anal. Biochem. **229:** 329–335.

Miranda, M., and Sorkin, A. (2007). Regulation of receptors and transporters by ubiquitination: New insights into surprisingly similar mechanisms. Mol. Interv. **7:** 157–167.

Nezames, C.D., and Deng, X.W. (2012). The COP9 signalosome: its regulation of cullin-based E3 ubiquitin ligases and role in photomorphogenesis. Plant Physiol. **160:** 38–46.

Qin, C., Qian, W., Wang, W., Wu, Y., Yu, C., Jiang, X., Wang, D., and Wu, P. (2008). GDP-mannose pyrophosphorylase is a genetic determinant of ammonium sensitivity in *Arabidopsis thaliana*. Proc. Natl. Acad. Sci. USA **105:** 18308–18313.

Saijo, Y., Sullivan, J.A., Wang, H., Yang, J., Shen, Y., Rubio, V., Ma, L., Hoecker, U., and Deng, X.W. (2003). The COP1-SPA1 interaction defines a critical step in phytochrome A-mediated regulation of HY5 activity. Genes Dev. **17:** 2642–2647.

Schwechheimer, C., and Isono, E. (2010). The COP9 signalosome and its role in plant development. Eur. J. Cell Biol. **89:** 157–162.

Seo, H.S., Yang, J.Y., Ishikawa, M., Bolle, C., Ballesteros, M.L., and Chua, N.H. (2003). LAF1 ubiquitination by COP1 controls photomorphogenesis and is stimulated by SPA1. Nature **423:** 995–999.

Smirnoff, N. (2000). Ascorbate biosynthesis and function in photoprotection. Philos. Trans. R. Soc. Lond. B Biol. Sci. **355:** 1455–1464.

Smirnoff, N., and Pallanca, J.E. (1996). Ascorbate metabolism in relation to oxidative stress. Biochem. Soc. Trans. **24:** 472–478.

Smirnoff, N., and Wheeler, G.L. (2000). Ascorbic acid in plants: Biosynthesis and function. Crit. Rev. Biochem. Mol. Biol. **35:** 291–314.

Tabata, K., Takaoka, T., and Esaka, M. (2002). Gene expression of ascorbic acid-related enzymes in tobacco. Phytochemistry **61:** 631–635.

Tajdoost, S., Farboodnia, T., and Heidari, R. (2007). Salt pretreatment enhance salt tolerance in *Zea mays* L. seedlings. Pak. J. Biol. Sci. **10:** 2086–2090.

Walter, M., Chaban, C., Schütze, K., Batistic, O., Weckermann, K., Näke, C., Blazevic, D., Grefen, C., Schumacher, K., Oecking, C., Harter, K., and Kudla, J. (2004). Visualization of protein interactions in living plant cells using bimolecular fluorescence complementation. Plant J. **40:** 428–438.

Wei, N., and Deng, X.W. (2003). The COP9 signalosome. Annu. Rev. Cell Dev. Biol. **19:** 261–286.

Wei, N., Serino, G., and Deng, X.W. (2008). The COP9 signalosome: More than a protease. Trends Biochem. Sci. **33:** 592–600.

Wheeler, G.L., Jones, M.A., and Smirnoff, N. (1998). The biosynthetic pathway of vitamin C in higher plants. Nature **393:** 365–369.

Wolucka, B.A., and Van Montagu, M. (2003). GDP-mannose 3′,5′-epimerase forms GDP-L-gulose, a putative intermediate for the *de novo* biosynthesis of vitamin C in plants. J. Biol. Chem. **278:** 47483–47490.

Yabuta, Y., Mieda, T., Rapolu, M., Nakamura, A., Motoki, T., Maruta, T., Yoshimura, K., Ishikawa, T., and Shigeoka, S. (2007). Light regulation of ascorbate biosynthesis is dependent on the photosynthetic electron transport chain but independent of sugars in *Arabidopsis*. J. Exp. Bot. **58:** 2661–2671.

Yang, J., Lin, R., Sullivan, J., Hoecker, U., Liu, B., Xu, L., Deng, X.W., and Wang, H. (2005). Light regulates COP1-mediated degradation of HFR1, a transcription factor essential for light signaling in *Arabidopsis*. Plant Cell **17:** 804–821.

Yoo, S.D., Cho, Y.H., and Sheen, J. (2007). *Arabidopsis* mesophyll protoplasts: a versatile cell system for transient gene expression analysis. Nat. Protoc. **2:** 1565–1572.

Zhang, W., Lorence, A., Gruszewski, H.A., Chevone, B.I., and Nessler, C.L. (2009). *AMR1*, an *Arabidopsis* gene that coordinately and negatively regulates the mannose/l-galactose ascorbic acid biosynthetic pathway. Plant Physiol. **150:** 942–950.

Zhang, Z., Wang, J., Zhang, R., and Huang, R. (2012). The ethylene response factor AtERF98 enhances tolerance to salt through the transcriptional activation of ascorbic acid synthesis in *Arabidopsis*. Plant J. **71:** 273–287.

Zhou, Z., Wang, Y., Cai, G., and He, Q. (2012). *Neurospora* COP9 signalosome integrity plays major roles for hyphal growth, conidial development, and circadian function. PLoS Genet. **8:** e1002712.